JACS
JOURNAL OF THE AMERICAN CHEMICAL SOCIETY
Communication
pubs.acs.org/JACS

Stereochemical Control of Polymorph Transitions in Nanoscale Reactors

Qi Jiang, Chunhua Hu, and Michael D. Ward*

Molecular Design Institute, Department of Chemistry, New York University, 100 Washington Square East, New York, New York 10003-6688, United States

Supporting Information

ABSTRACT: Crystallization of glycine in the cylindrical nanopores of anodic aluminum oxide (AAO) revealed the formation of metastable β-glycine in pores having diameters less than 200 nm. Two-dimensional X-ray microdiffraction indicated that the [010] axis of the embedded β-glycine nanocrystals coincided with the pore direction, identical to behavior observed previously in the cylindrical nanopores of polymer monoliths. Whereas the β-glycine nanocrystals were stable indefinitely in ambient air and persisted upon heating, they transformed to the α polymorph upon standing at room temperature and 90% relative humidity (RH). The α-glycine nanocrystals were oriented with the [010] axis nearly perpendicular to the pore direction, reflecting a nearly 90° rotation of the glycine molecules during the transition. When the β-glycine nanocrystals were formed in the AAO cylinders in the presence of small amounts of racemic hydrophobic amino acid auxiliaries, which are known to bind selectively to the (010) and (0$\bar{1}$0) faces on the fast-growing end of β-glycine enantiomorphs, the $\beta \rightarrow \alpha$ phase transition at 90% RH was suppressed. In contrast, β-glycine nanocrystals grown in the presence of an enantiopure amino acid auxiliary, which binds to the fast-growing end of only one of the enantiomorphs, thus suppressing its formation and leaving the other enantiomorph unperturbed, transformed into the α polymorph under the same conditions. This observation confirms that binding of an amino acid to the {010} faces is stereoselective and that access of water to these faces is essential for the transition to the α polymorph.

Polymorphism, the ability of a compound to adopt multiple crystalline forms,[1] is increasingly becoming recognized as a considerable fundamental and technological challenge in solid-state chemistry, organic materials, and pharmaceutical science.[2−4] Glycine, the simplest amino acid, has emerged as an exceptionally interesting platform for investigating polymorphism, as it exists in three forms under ambient conditions.[5] Examination of the phase transitions between these forms has revealed a stability ranking $\gamma > \alpha > \beta$.[6,7] Whereas the α polymorph forms most readily when glycine is crystallized from aqueous solutions, the β polymorph can be crystallized by the addition of methanol or ethanol to aqueous solutions, and the γ polymorph grows in acidified aqueous solutions. Although a limited number of studies have been performed to unravel the mechanisms responsible for the crystallization of these polymorphs,[8] the transitions are not well understood at the molecular level. Herein we report the transition of glycine polymorphs under confinement within the cylindrical pores of anodic aluminum oxide (AAO) and the role of stereochemical auxiliaries on this $\beta \rightarrow \alpha$ phase transition.

Recently, the crystallization of glycine within cylindrical nanoscale pores in polymer monoliths revealed that formation of the metastable β polymorph was favored in pores having small diameters (<30 nm).[9] The formation of β-glycine also was favored in micrometer-scale wells on patterned substrates.[10,11] In the polymer monoliths, two-dimensional X-ray microdiffraction (2D μ-XRD) indicated that the β-glycine crystals, which exhibit a needlelike morphology in the bulk, were oriented with the fast-growth [010] axis coinciding with the pore direction. β-Glycine is chiral and therefore exists as two enantiomorphs ($P2_1$ space group). The crystals have a needlelike habit with one end tapered to a point, indicative of vanishingly small (010) and (0$\bar{1}$0) faces at the fast-growing crystal tips of the two enantiomorphs, assigned as (010) for the (+)-β enantiomorph and (0$\bar{1}$0) for the (−)-β enantiomorph. Racemic mixtures of chiral auxiliaries [(*R*,*S*)-phenylalanine, (*R*,*S*)-methionine, and (*R*,*S*)-tryptophan] block the growth of β-glycine along the *b* axis because of enantioselective binding to the (010) (+)-β and (0$\bar{1}$0) (−)-β faces.[12] This affords a change of crystal habit from needles to plates with large {010} faces. When crystallization was conducted within the polymer monolith nanopores in the presence of racemic mixtures of these auxiliaries, the β-glycine crystals grew with their *b* axis perpendicular to the cylinder axis, that is, rotated by 90° compared with the orientation observed in the absence of the auxiliaries. In contrast, when β-glycine was crystallized in the nanopores in the presence of an enantiopure auxiliary, the crystal orientation was identical to that observed in the absence of the auxiliaries. This observation demonstrated that an enantiopure auxiliary inhibits the growth of only one of the enantiomorphs through specific binding, allowing the unaffected enantiomorph to grow unimpeded with the [010] axis parallel with the pore direction. The unique crystal growth behavior of glycine and other organic crystals in nanoporous polymer monoliths[13] prompted us to examine crystallization of a variety of materials, including glycine, in the cylindrical nanopores of AAO.[14] Although crystallization of polymers

Received: December 21, 2012
Published: January 31, 2013

dx.doi.org/10.1021/ja312511v | *J. Am. Chem. Soc.* 2013, 135, 2144−2147

embedded in AAO has been reported,[15] the growth and phase behavior of molecular crystals in AAO has not.

Glycine was introduced to AAO nanopores with diameters ranging from 20 to 200 nm by immersion of a 60 μm thick AAO membrane in an aqueous solution containing 18 wt % glycine followed by removal of the water by vacuum drying at ambient temperature. The surfaces of the AAO membrane were carefully swabbed with a wet tissue to remove any bulk glycine residue on the surface. The embedded glycine crystals were characterized on a Bruker GADDS X-ray microdiffractometer equipped with a 2D area detector capable of simultaneous determination of phase and orientation[16] using a beam diameter collimated to 0.5 mm [see Figure S1 in the Supporting Information (SI)]. Whereas a random orientation of the population of embedded crystals would generate continuous arcs on the detector at values of 2θ corresponding to allowed (hkl) reflections, the glycine crystals exhibited discontinuous arcs that signaled a preferred orientation within the cylindrical AAO pores. The preferred crystal orientation was determined by measurement of the positions of the diffraction arcs $(2\theta, \delta)$ on the 2D detector at a particular incident X-ray beam angle (θ_1) followed by an analysis using eq 1 to determine a self-consistent set of dihedral angles (Φ) between individual Miller planes $(h_nk_nl_n)$ and a reference plane $(h_1k_1l_1)$, which was chosen as the plane with an average orientation perpendicular to the pore direction (see Figure S2).

$$\cos\Phi = \sin\theta \sin\theta_1 + \cos\theta \cos\theta_1 \cos\delta \quad (1)$$

Glycine initially crystallized as the β polymorph within the AAO nanocylinders, in agreement with crystallization in the aforementioned nanoporous polymer monoliths. Analysis of the 2D diffraction patterns revealed that, on average, the (020) planes of β-glycine were perpendicular to the cylindrical pore axis ($2\theta = 28.5°$; $\delta = 0°$) and the (001) planes were parallel to the pore axis ($2\theta = 17.9°$; $\delta = 90°$) (Figure 1A and Table S1 in the SI). Bulk crystals of β-glycine readily transform to α-glycine in humid air upon standing for hours at room temperature[5b] or rapidly upon heating to 67 °C.[7a] In contrast, β-glycine nanocrystals embedded in the AAO cylinders were stable indefinitely upon standing in ambient air, and they did not transform to α-glycine even upon heating to 200 °C, where they decompose. However, after exposure to 90% relative humidity (RH) for 24 h at ambient temperature, the embedded β-glycine nanocrystals transformed to α-glycine ($P2_1/n$ space group; Figure 1B). The 2D diffraction pattern indicated that the (020) planes and (20$\bar{1}$) planes of α-glycine were parallel and perpendicular to the pore axis, respectively, consistent with the [100] axis coinciding with the pore direction (Figure S3 and Table S2). This orientation was corroborated by the positions of the (110) and (120) reflections on the detector. Comparison of the solid-state structures of the two polymorphs revealed that the orientation of the newly formed α-glycine crystals corresponded to 90° rotation of the glycine molecules within the experimental Cartesian frame relative to their orientation in the original β-glycine crystals (Figure 2).

XRD measurements of the temporal evolution of the $\beta \rightarrow \alpha$ phase transition in AAO under 90% RH (Figure S4) demonstrated a gradual decrease in β-glycine with a concomitant increase in α-glycine (Figure S5). Notably, addition of a water droplet to the surface of an AAO membrane with embedded β-glycine nanocrystals resulted in an immediate decrease in the diffraction intensity from β-glycine followed by a gradual recrystallization of embedded β-glycine upon drying

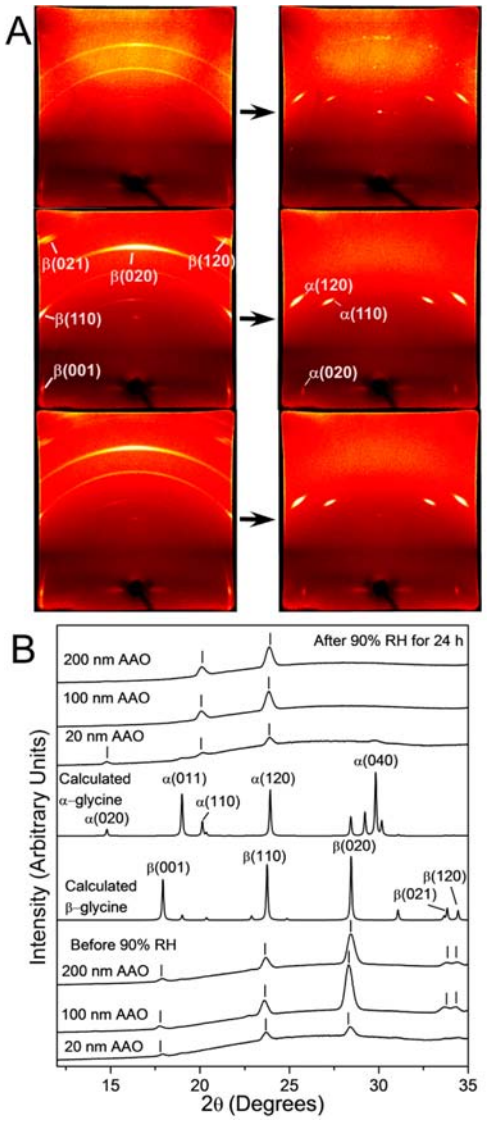

Figure 1. (A) 2D μ-XRD patterns of glycine embedded in (top) 20 nm, (middle) 100 nm, and (bottom) 200 nm AAO, revealing the transition from the initially formed β-glycine (left column) to its α form (right column) after exposure to 90% relative humidity (RH) for 24 h. The discontinuous diffraction arcs signal preferential orientations of the glycine crystals. (B) 1D μ-XRD patterns for embedded glycine crystals before and after the $\beta \rightarrow \alpha$ phase transition.

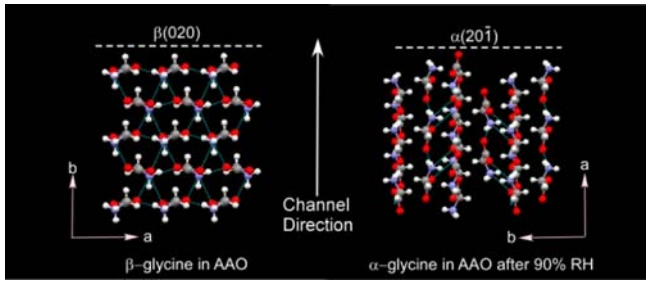

Figure 2. Molecular packing with respect to the AAO pore direction of (left) β-glycine to (right) α-glycine before and after the $\beta \rightarrow \alpha$ phase transition, respectively.

(Figure S6). These observations demonstrate that exposure to 90% RH does not result in dissolution of the embedded β-glycine nanocrystals, as this should produce β-glycine upon

dx.doi.org/10.1021/ja312511v | J. Am. Chem. Soc. 2013, 135, 2144−2147

drying. Instead, the results suggest that the $\beta \rightarrow \alpha$ phase transition is triggered by an interfacial reaction between water vapor and the crystal surfaces, which would produce defects that permit a solid-state phase transition.

The $\beta \rightarrow \alpha$ phase transition in AAO observed under 90% RH prompted us to examine the influence of chiral auxiliaries, which as mentioned above are known to bind to the (010) and $(0\bar{1}0)$ faces at the fast-growing crystal tips of the two β-glycine enantiomorphs. In the presence of racemic D,L-phenylalanine (D,L-Phe), the β-glycine crystals grew in the AAO pores with their [001] direction (rather than [010]) aligned with the pores, mirroring the behavior observed previously in nanoporous polymer monoliths.[9b] Interestingly, AAO-embedded β-glycine crystals grown in this manner did not transform into the α form when exposed to 90% RH. (Figure 3A–C) The phase

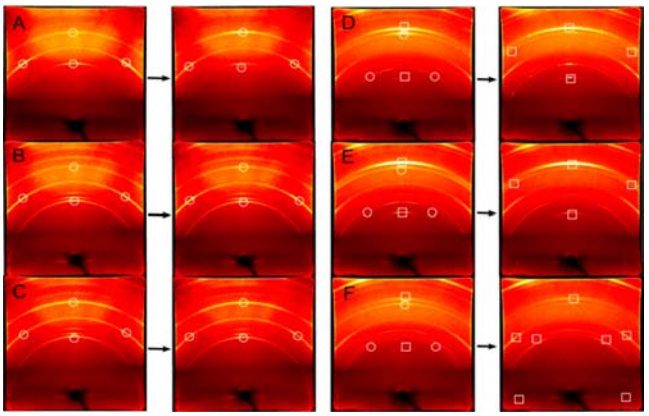

Figure 3. (A–C) 2D μ-XRD patterns for β-glycine crystals grown in the presence of racemic D,L-Phe (1.2 wt % in water) in (A) 20 nm, (B) 100 nm, and (C) 200 nm AAO (left) before and (right) after exposure to 90% RH for 24 h. (D–F) 2D μ-XRD patterns for β-glycine crystals grown in the presence of L-Phe (1.2 wt % in water) in (D) 20 nm, (E) 100 nm, and (F) 200 nm AAO (left) before and (right) after 90% RH for 24 h. The discontinuous diffraction arcs highlighted by circles (○) and squares (□) correspond to β-glycine and α-glycine, respectively.

transition also was suppressed for β-glycine nanocrystals grown in the presence of D,L-tryptophan (D,L-Trp) or D,L-methionine (D,L-Met), although in these cases the embedded β-glycine nanocrystals exhibited the [010] orientation (Figure S7).

When the β-glycine nanocrystals were grown in the presence of *enantiopure* auxiliaries, such as L-tryptophan (L-Trp), the $\beta \rightarrow \alpha$ phase transition was observed. This behavior can be attributed to the existence of a single enantiomorph whose growth was unaffected by stereochemical binding, resulting in a crystal with a (010) face unprotected by an auxiliary. Similar behavior was observed for β-glycine nanocrystals grown in the presence of L-glutamic acid (L-Glu). For nanocrystals grown in the presence of L-phenylalanine (L-Phe), the $\beta \rightarrow \alpha$ phase transition was observed (Figure 3D–F). In the presence of L-Phe or L-Met, both the α and β forms crystallized in the AAO pores initially, each with their [010] axes coinciding with the pore direction. The β nanocrystal fraction transformed to α under 90% RH; the orientation of the resulting α-glycine nanocrystals was identical to that observed for the $\beta \rightarrow \alpha$ phase transition when β was the only phase embedded in AAO. The initial α fraction, however, retained its [010] orientation parallel to the pore.

Of the 20 amino acids, only racemic phenylalanine, tryptophan, methionine, and glutamic acid suppressed the $\beta \rightarrow \alpha$ phase transition of the embedded glycine nanocrystals (Table 1). With the exception of glutamic acid, these are the

Table 1. Polymorphs and Orientations of Glycine Crystals Embedded in AAO before and after the Polymorphic Transition

		glycine polymorph and direction parallel to the pore direction[b]	
auxiliary[a]	wt % in water	initial crystallization	after 90% RH for 24 h
none	–	β [010]	α [100]
D,L-Phe	1.2	β [001]	β [001]
D,L-Trp	0.3	β [010]	β [010]
D,L-Met	1.2	β [010]	β [010]
D,L-Glu	1.2	β, random	β, random
D,L-Ala	1.2	β [010]	α [100]
D,L-Val	1.2	β [010]	α [100]
D,L-Leu	0.3	β [010]	β [010] + α [100][e]
D,L-His	1.2	β [001]	β [001] + α [100][f]
D,L-Ser	1.2	β [010]	β [001] + α [100][e]
D,L-Pro	1.2	β [010]	α [100]
L-Phe	1.2	β [010] + α [010]	α [010] + α [100][e]
L-Trp	0.3	β [010]	α [100]
L-Met	1.2	β [010] + α [010]	α [010] + α [100][e]
L-Glu	1.2	β [001][c]	α [100]
L-Ala	1.2	β [010]	α [100]
L-Val	1.2	β [010]	α [100]
L-Leu	0.3	β [010] + α [010]	α [010] + α [100][e]
L-His	1.2	β [001]	α [100][g]
L-Ser	1.2	β [001][c]	α [100]
L-Pro	1.2	β [001] + α [010][d]	α [100][e]

[a]Abbreviations: Phe, phenylalanine; Trp, tryptophan; Met, methionine; Glu, glutamic acid; Ala, alanine; Val, valine; Leu, leucine; His, histidine; Ser, serine; Pro, proline. [b]The glycine orientation was determined by 2D μ-XRD data for 20, 100, and 200 nm AAO membranes, and some samples had two polymorphs or two different orientations as well as random orientations (Table S3). [c]In 20 nm AAO, β [010]. [d]In 20 nm AAO, β [010] + α [010]. [e]In 20 nm AAO, α [010]. [f]In 20 nm AAO, α [100]. [g]In 20 nm AAO, α, random.

most hydrophobic of the amino acids, and they have bulky side chains (Figure S8). Racemic auxiliaries with short, hydrophilic side chains [e.g., alanine (Ala) or serine (Ser)] did not suppress the $\beta \rightarrow \alpha$ transition. Investigations with other amino acids were precluded by their poor solubility in water (<1 wt %) (Table S4). The data suggest that the stereospecific binding of bulky racemic auxiliaries (hydrophobic ones in particular) to the {010} planes of β-glycine is crucial for suppressing the $\beta \rightarrow \alpha$ phase transition, regardless of the initial orientation of β-glycine nanocrystals in the pore (Figure 4). Furthermore, these observations are consistent with a phase transition driven by an interfacial reaction between water and the polar {010} faces at the tips of the β-glycine crystals.

These studies further illustrate that the investigation of crystalline compounds under nanoscale confinement continues to provide new insights into the behavior of polymorphs and their phase behaviors. The reactivity of the polar {010} faces of β-glycine nanocrystals is consistent with a surface-mediated nucleation and growth mechanism.[17] The suppression of the $\beta \rightarrow \alpha$ transition by racemic auxiliaries known to bind selectively to the {010} faces of β-glycine implies a surprising specificity for the reaction of water with the {010} faces relative to other exposed faces. Moreover, the stabilization of a chiral crystalline phase by stereochemical binding of additives suggests a possible

dx.doi.org/10.1021/ja312511v | J. Am. Chem. Soc. 2013, 135, 2144–2147

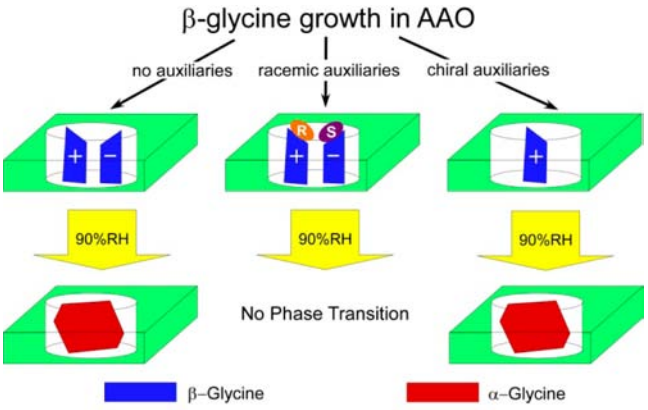

Figure 4. Illustration of the preferred orientation and phase transitions of glycine crystals in AAO cylindrical pores after exposure to 90% RH. In the absence of auxiliaries, *β*-glycine transforms to *α*-glycine. *β*-Glycine crystals grown in the presence of racemic auxiliaries do not transform because of enantioselective binding of the auxiliaries to the fast-growing tips of the *β*-glycine crystal. When grown in the presence of an enantiopure auxiliary, one enantiomorph survives [shown here as the (+) enantiomorph] and transforms to *α*-glycine at 90% RH.

mechanism for the preservation of biological homochirality in crystalline form that may have been important in chirality amplification in primordial times.[18]

■ ASSOCIATED CONTENT

Supporting Information

Materials and experimental details for characterization of XRD and nanocrystal orientation analysis. This material is available free of charge via the Internet at http://pubs.acs.org.

■ AUTHOR INFORMATION

Corresponding Author

mdw3@nyu.edu

Notes

The authors declare no competing financial interest.

■ ACKNOWLEDGMENTS

The work was supported by the National Science Foundation (NSF) Chemical Research Instrumentation and Facilities Program under Award CRIF/CHE-0840277 and by the NSF Materials Research Science and Engineering Centers Program under Award MRSEC/DMR-0820341. The authors thank Dr. Stephanie S. Lee for helpful comments and the NYU Molecular Design Institute for support.

■ REFERENCES

(1) Bernstein, J. *Polymorphism in Molecular Crystals*; Oxford University Press: New York, 2002.
(2) Bond, A. D. *Curr. Opin. Solid State Mater. Sci.* **2009**, *13*, 91.
(3) Vippagunta, S. R.; Brittain, H. G.; Grant, D. J. W. *Adv. Drug Delivery Rev.* **2001**, *48*, 3.
(4) Valeev, E. F.; Coropceanu, V.; da Silva Filho, D. A.; Salman, S.; Brédas, J.-L. *J. Am. Chem. Soc.* **2006**, *128*, 9882.
(5) (a) Marsh, R. E. *Acta Crystallogr.* **1958**, *11*, 654. (b) Iitaka, Y. *Acta Crystallogr.* **1960**, *13*, 35. (c) Iitaka, Y. *Acta Crystallogr.* **1961**, *14*, 1.
(6) (a) Chongprasert, S.; Knopp, S. A.; Nail, S. L. *J. Pharm. Sci.* **2001**, *90*, 1720. (b) Boldyreva, E. V.; Drebushchak, V. A.; Drebushchak, T. N.; Paukov, I. E.; Kovalevskaya, Y. A.; Shutova, E. S. *J. Therm. Anal. Calorim.* **2003**, *73*, 409.
(7) (a) Boldyreva, E. V.; Drebushchak, V. A.; Drebushchak, T. N.; Paukov, I. E.; Kovalevskaya, Y. A.; Shutova, E. S. *J. Therm. Anal. Calorim.* **2003**, *73*, 419. (b) Allen, K.; Davey, R. J.; Ferrari, E.; Towler, C.; Tiddy, G. J.; Jones, M. O.; Pritchard, R. G. *Cryst. Growth Des.* **2002**, *2*, 523. (c) Weissbuch, I.; Leiserowitz, L.; Lahav, M. *Adv. Mater.* **1994**, *6*, 952.
(8) (a) Weissbuch, I.; Addadi, L.; Lahav, M.; Leiserowitz, L. *Science* **1991**, *253*, 637. (b) Weissbuch, I.; Torbeev, V. Yu.; Leiserowitz, L.; Lahav, M. *Angew. Chem., Int. Ed.* **2005**, *44*, 3226. (c) Huang, J.; Stringfellow, T. C.; Yu, L. *J. Am. Chem. Soc.* **2008**, *130*, 13973.
(9) (a) Hamilton, B. D.; Hillmyer, M. A.; Ward, M. D. *Cryst. Growth Des.* **2008**, *8*, 3368. (b) Hamilton, B. D.; Weissbuch, I.; Lahav, M.; Hillmyer, M. A.; Ward, M. D. *J. Am. Chem. Soc.* **2009**, *131*, 2588.
(10) Lee, A. Y.; Lee, I. S.; Dette, S. S.; Boerner, J.; Myerson, A. S. *J. Am. Chem. Soc.* **2005**, *127*, 14982.
(11) Kim, K.; Lee, I. S.; Centrone, A.; Hatton, T. A.; Myerson, A. S. *J. Am. Chem. Soc.* **2009**, *131*, 18212.
(12) Torbeev, V. Yu.; Shavit, E.; Weissbuch, I.; Leiserowitz, L.; Lahav, M. *Cryst. Growth. Des.* **2005**, *5*, 2190.
(13) (a) Ha, J.-M.; Wolf, J. H.; Hillmyer, M. A.; Ward, M. D. *J. Am. Chem. Soc.* **2004**, *126*, 3382. (b) Ha, J.-M.; Hamilton, B. D.; Hillmyer, M. A.; Ward, M. D. *Cryst. Growth Des.* **2009**, *9*, 4766. (c) Ha, J.-M.; Hamilton, B. D.; Hillmyer, M. A.; Ward, M. D. *Cryst. Growth Des.* **2012**, *12*, 4494. (d) Hamilton, B. D.; Ha, J.-M.; Hillmyer, M. A.; Ward, M. D. *Acc. Chem. Res.* **2012**, *45*, 412.
(14) (a) Masuda, H.; Fukuda, K. *Science* **1995**, *268*, 1466. (b) *Ordered Porous Nanostructures and Applications*; Wehrspohn, R. B., Ed.; Springer: New York, 2005.
(15) (a) Steinhart, M.; Stephan, S.; Wehrspohn, R. B.; Gösele, U.; Wendorff, J. H. *Macromolecules* **2003**, *36*, 3646. (b) Steinhart, M.; Göring, P.; Dernaika, H.; Prabhukara, M.; Gösele, U.; Hempel, E.; Thurn-Albrecht, T. *Phys. Rev. Lett.* **2006**, *97*, No. 027801. (c) Wu, H.; Wang, W.; Yang, H.; Su, Z. *Macromolecules* **2007**, *40*, 4244. (d) Wu, H.; Wang, W.; Huang, Y.; Wang, C.; Su, Z. *Macromolecules* **2008**, *41*, 7755. (e) Wu, H.; Wang, W.; Huang, Y.; Su, Z. *Macromol. Rapid Commun.* **2009**, *30*, 194. (f) Serghei, A.; Lutkenhaus, J. L.; Miranda, D. F.; McEnnis, K.; Kremer, F.; Russell, T. P. *Small* **2010**, *6*, 1822. (g) García-Gutiérrez, M.-C.; Linares, A.; Hernández, J. J.; Rueda, D. R.; Ezquerra, T. A.; Poza, P.; Davies, R. J. *Nano Lett.* **2010**, *10*, 1472. (h) Michell, R. M.; Lorenzo, A. T.; Müller, A. J.; Lin, M.-C.; Chen, H.-L.; Blaszczyk-Lezak, I.; Martin, J.; Mijangos, C. *Macromolecules* **2012**, *45*, 1517.
(16) He, B. B. *Two Dimensional X-Ray Diffraction*; Wiley: New York, 2009.
(17) Beckham, G. T.; Peters, B.; Starbuck, C.; Variankaval, N.; Trout, B. L. *J. Am. Chem. Soc.* **2007**, *129*, 4714.
(18) Weissbuch, I.; Leiserowitz, L.; Lahav, M. *Top. Curr. Chem.* **2005**, *259*, 123.